Supporting Information

Monje et al. 10.1073/pnas.1101657108

SI Materials and Methods

Case Selection and Quality Control. Fifty-one cases were identified in the neuropathology archives at a single institution (Stanford University) in which the brain was described as having no abnormality on neuropathological examination, and the subjects had no history of neurodevelopmental or oncological disease. All samples were collected during the course of a routine brain autopsy protocol that includes sampling of various brain regions. Of note, one of the regions routinely sampled is the hippocampus, which is exquisitely sensitive to hypoxic/ischemic events. Cases were excluded if there was evidence of hypoxia/ischemia in the hippocampus or elsewhere, because such neuropathological insults can affect immunophenotypic marker expression. Following tissue quality assessment, 24 of these cases were included in this study, with patients ranging in age from 3 mo to 18 y of life. Tissue quality was assessed based on immunoreactivity for Olig2 in white matter tracts and Nestin in blood vessels; only those samples with strong staining in the expected patterns were included in this study. Formalin-fixed, paraffin-embedded tissue sections were prepared from the midbrain, pons, and medulla of these 24 cases for immunohistochemical analysis.

Tissue Donor. The tumor tissue donor was a 5-y-old boy with a large (~5 cm) diffuse intrinsic pontine tumor. He received minimal treatment for the tumor, beginning radiation therapy but stopping after only 3 fractions of a planned 30-fraction course of radiotherapy (he received a total dose 5.4 Gy in 3 fractions of 1.8 Gy each). He received glucocorticoid therapy to minimize edema but did not receive chemotherapy, and he died within 2 mo of his diagnosis. Tumor harvest occurred 14 h after the time of death under sterile conditions in the autopsy suite with informed consent from the family and approval from the institutional review board.

Primary Tumor Cell Culture. Tumor tissue was harvested under sterile conditions in the autopsy suite, collected in serum-free DMEM/12 (Cellgro), and transported on ice to the laboratory. The tissue was then minced with a sterile no. 10 scalpel and washed twice in Hepes-HBSS (HeHBSS) to remove debris. Minced tissue was then added to dissociation buffer (HeHBSS) with DNaseI (250 U/mL) and collagenase type IV (1 mg/mL). Minimal mechanical force was used, and the cells were allowed to dissociate at 37 °C on a Nutator (Fisher Scientific). The cells were sequentially strained through 100-, 70-, and 40-μm cell strainers and then centrifuged and processed through a sucrose gradient. Dissociated cells were treated with red blood cell lysis buffer (Invitrogen) and plated at subclonal density of 100 cells/mL for neurosphere formation in tumor stem media (TSM) consisting of Neurobasal(-A) (Invitrogen), B27(-A) (Invitrogen), human-basic FGF (20 ng/mL; Shenandoah Biotech), human-EGF (20 ng/mL; Shenandoah Biotech), human PDGF-AB (20 ng/mL; Shenandoah Biotech), and heparin (10 ng/mL).

Immunohistochemistry, Immunocytochemistry, and Confocal Microscopy. Immunocytochemical staining of tumor cells was performed in poly-D-lysine and laminin-coated glass chamber slides following fixation with 4% (wt/vol) paraformaldehyde. Floating tissue sections were used for mouse tissue following fixation with 4% (wt/vol) paraformaldehyde and preparation on a sliding microtome. Formalin-fixed, paraffin-embedded human tissue was deparaffinized, and microwave antigen retrieval was performed using either citrate buffer for Nestin, Vimentin, and GFAP antibodies (pH 6.0; Dako) or EDTA buffer for Olig2 antibody (pH 9.0; Dako). Immunostaining was performed as described (1) using the following primary antibodies and working concentrations: anti-GFAP (rabbit, 1:500; Dako), anti-Nestin (mouse, 1:1,000; Millipore), anti-Nestin (rabbit, 1:500; Covance), anti-Vimentin (mouse, 1:500; Dako), anti-SOX2 (goat, 1:50; R&D Systems), anti-Olig2 (rabbit, 1:500; Millipore), anti-Ki67 (rabbit, 1:25; Abcam), and anti-CD133 (mouse, 1:50; Miltenyi Biotechnology).

All confocal microscopy was performed using a Zeiss 510 confocal microscope. Appropriate gain and black level settings was determined on control tissues stained with secondary antibodies alone. Upper and lower thresholds were always set using the range indicator function to minimize data loss through saturation. For quantification of marker colocalization, at least 100 cells per sample were scored whenever possible using confocal microscopy.

Stereological Quantification and Cell Counting. A one in four series of 40-μm sections throughout the rostrocaudal extent of the murine pontomedulla was immunostained as described above. All sections that contain the IVth ventricle dorsally were included. One side (right or left) of this symmetrical structure was analyzed in each animal. The total number of immunopositive cells in the ventral hemipons was quantified at a magnification of 20× on a fluorescent microscope by an investigator blinded to experimental conditions. In each section of this one in four series, 100% of the ventral pontine area was quantified and the total number of cells counted was multiplied by 4 to account for the intervening sections.

FACS. Neurosphere cells were dissociated and then incubated with anti-CD133/1-allophycocyanin (APC) and anti-CD133/2 mouse monoclonal antibody directly conjugated with the fluorophore APC (mouse, 1:50; Miltenyi Biotechnology). Analysis was performed on an LSR flow cytometer (BD Biosciences) at the Stanford University FACS facility. IgG1A and IgG2B directly conjugated to APC were used as controls for nonspecific isotype background staining. For isolation and plating of live cells, dissociated neurosphere cells were stained with propidium iodide and sorted on an ARIA-II FACS machine (BD Biosciences); 100 cells per well were directly plated into a 96-well uncoated tissue culture plate.

Stereotactic Transplantation. Nonobese diabetic/SCID/γ-chain null–immunodeficient mice were used in accordance with approved institutional animal use and care protocols. In total, 40,000 live tumor cells (2-μL volume of 20,000 cells/μL) were transplanted into the LVs, or 200,000 live tumor cells (2-μL volume of 100,000 cells/μL) were transplanted into the IVth ventricle of cold-anesthetized P2 mouse pups by stereotactic injection through a 31-gauge burr hole (coordinates: 2 mm anterior to the bregma, 1 mm lateral to the sagittal suture, and 2 mm deep for the LV; 3 mm posterior to the λ-suture and 3 mm deep for the IVth ventricle.) Mice were returned to the mother until weaned, monitored for sickness behavior, and killed at 6 mo of age.

Limiting Dilution and Analysis of Neurosphere Formation. For estimation of sphere-initiating cell frequency, limiting dilution analysis was done as described previously (2, 3). Dissociated cells were plated in limiting doses. Cultures were carried for 9–12 wk and scored for wells that did not have neurospheres. An extreme limiting-dilution analysis algorithm was used to determine the

frequency of gliomasphere renewing cells (4). Analyses were performed, using the limdil function of the "StatMod" package part of the R statistical software project (http://www.r-project.org) (5).

Generation of Lenti-Based Gli-RFP Reporter. Gli luciferase reporter constructs 8 × 3′Gli BSwt-luc and 8 × 3′Gli BSmut-luc were provided by Hiroshi Sasaki (Center for Developmental Biology, RIKEN, Kobe, Japan) (6). The Gli binding site cassette was amplified along with a thymidine kinase (TK) basic promoter and inserted upstream of GFP into the lentiviral transfer vector pRRL.sin-18.PPT.GFP.pre (7). The GFP cDNA was then excised and replaced with that coding for monomeric RFP (mRFP) (from pRSET-B mRFP; a gift of Roger Tsien, University of California, San Diego, CA) to generate the lentivirus-based Gli-RFP reporter.

Real-Time PCR. Dissociated DIPG neurospheres were grown in TSM in a six-well plate (200,000 cells per well). RNA was extracted and purified using PureLink RNA Mini columns (Invitrogen) according to the manufacturer's instructions. Superscript III reverse transcriptase (Invitrogen) was used to make cDNA from RNA. Real-time PCR of cDNA was performed on a BioRad iCycler. Hypoxanthine phosphoribosyltransferase 1 (HPRT1) was used as the internal reference gene. Results are given as a normalized expression relative to the mean expression of the DLD-1 cancer cell line (2^{-DDCt}).

PCR primers were as follows:

Gli1: forward primer (5′–3′), GAAGTCATACTCACGCCTC GAA; reverse primer (5′–3′), CAGCCAGGGAGCTTA CATACAT
Ptch: forward primer (5′–3′), GGACACTCTCATCTTTTG CTG; reverse primer (5′–3′), GGTAGTCTGCTTTCTG GGT
Shh: forward primer (5′–3′), CAAGCAGTTTATCCCCAAT GTG; reverse primer (5′–3′), TCACCCGCAGTTTCA CTC
HPRT1: forward primer (5′–3′), GGTCAGGCAGTATAAT CCAAAG; reverse primer (5′–3′), GGACTCCAGATG TTTCCAAAC

Statistics. Unpaired, two-tailed Student *t* tests were used in all comparisons.

1. Palmer TD, Willhoite AR, Gage FH (2000) Vascular niche for adult hippocampal neurogenesis. *J Comp Neurol* 425:479–494.
2. Singh SK, et al. (2003) Identification of a cancer stem cell in human brain tumors. *Cancer Res* 63:5821–5828.
3. Uchida N, et al. (2000) Direct isolation of human central nervous system stem cells. *Proc Natl Acad Sci USA* 97:14720–14725.
4. Hu Y, Smyth GK (2009) ELDA: extreme limiting dilution analysis for comparing depleted and enriched populations in stem cell and other assays. *J Immunol Methods* 347:70–78.
5. Bonnefoix T, Bonnefoix P, Verdiel P, Sotto JJ (1996) Fitting limiting dilution experiments with generalized linear models results in a test of the single-hit Poisson assumption. *Journal Immunol Methods* 194:113–119.
6. Sasaki H, Hui C, Nakafuku M, Kondoh H (1997) A binding site for Gli proteins is essential for HNF-3beta floor plate enhancer activity in transgenics and can respond to Shh in vitro. *Development* 124:1313–1322.
7. Follenzi A, Ailles LE, Bakovic S, Geuna M, Naldini L (2000) Gene transfer by lentiviral vectors is limited by nuclear translocation and rescued by HIV-1 pol sequences. *Nat Genet* 25:217–222.

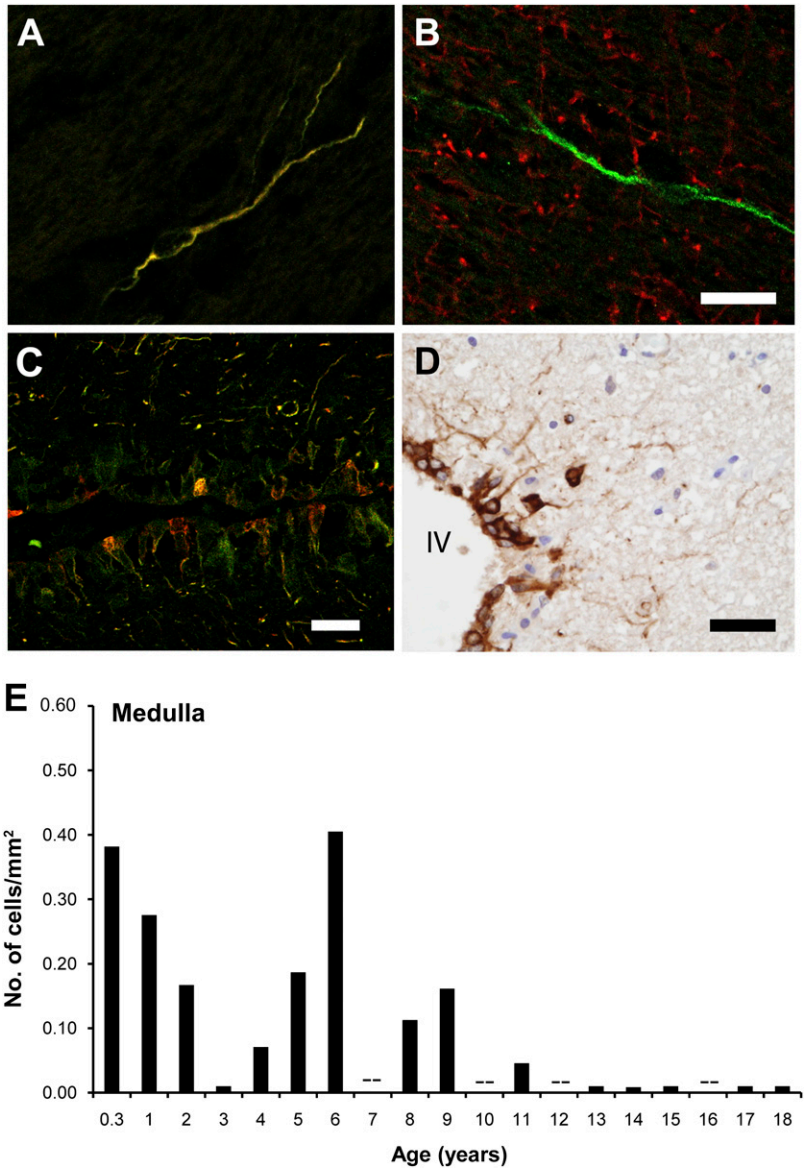

Fig. S1. Characterization of human brainstem precursor-like cells. Confocal photomicrographs (magnification 40×) of Nestin-immunopositive cells (green) in the ventral pons of a 6-y-old girl that coexpress Vimentin (*A*, red) but not GFAP (*B*, red). (Scale bar: 30 μm.) (*C*) Confocal micrograph (magnification 40×) of Nestin (green) and Vimentin (red) expression in the human IVth ventricle subventricular zone. (Scale bar: 20 μm.) (*D*) Light micrograph (magnification 40×) of the human IVth ventricle in a 5-y-old girl, at the level of the dorsal pons, showing Nestin-immunopositive cells (brown). Note that the globular teardrop morphology of the IVth ventricle subventricular zone cells shown here is distinct from the elongated bipolar morphology of Nestin$^+$ cells in the ventral brainstem in *A* and *B*. A subset of ependymal cells is also Nestin-immunopositive, and the majority of ependymal cells visible in this image express Nestin. (Scale bar: 50 μm.) (*E*) Density of Nestin-immunoreactive cells in the human ventral medulla as a function of postnatal age (n = 20). Each data point represents one to two cases. The symbol (--) denotes an age at which no valid tissue samples were available for analysis.

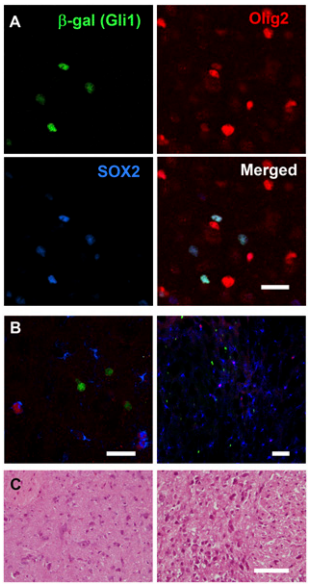

Fig. S2. Mouse brainstem. (*A*) Confocal micrograph (z-stack projection image) illustrating colocalization of Olig2 (red), SOX2 (blue), and β-galactosidase [indicating Gli1 expression (green)] (magnification 40× magnification). (Scale bar: 20 μm.) (*B*) Confocal micrographs illustrating PDGFR-α–immunopositive (blue) oligodendrocyte precursor cells that are dividing (Ki67, red) intermixed with β-galactosidase (Gli1)–expressing cells (green) in the ventral pons at P21 of a *Gli1::LacZ* mouse (magnification: *Left*, 40×; *Right*, 20×). These images are taken from the pontine region marked by an asterisk in Fig. 2*C*. (Scale bars: *Left*, 30 μm; *Right*, 50 μm.) (*C*) Light micrograph (magnification 20×) illustrating H&E-stained sections of the pons at P21 in control (*Left*) and *Olig2-Cre; R26-lsl-SmoM2* (*Right*) mice. (Scale bar: 200 μm.)

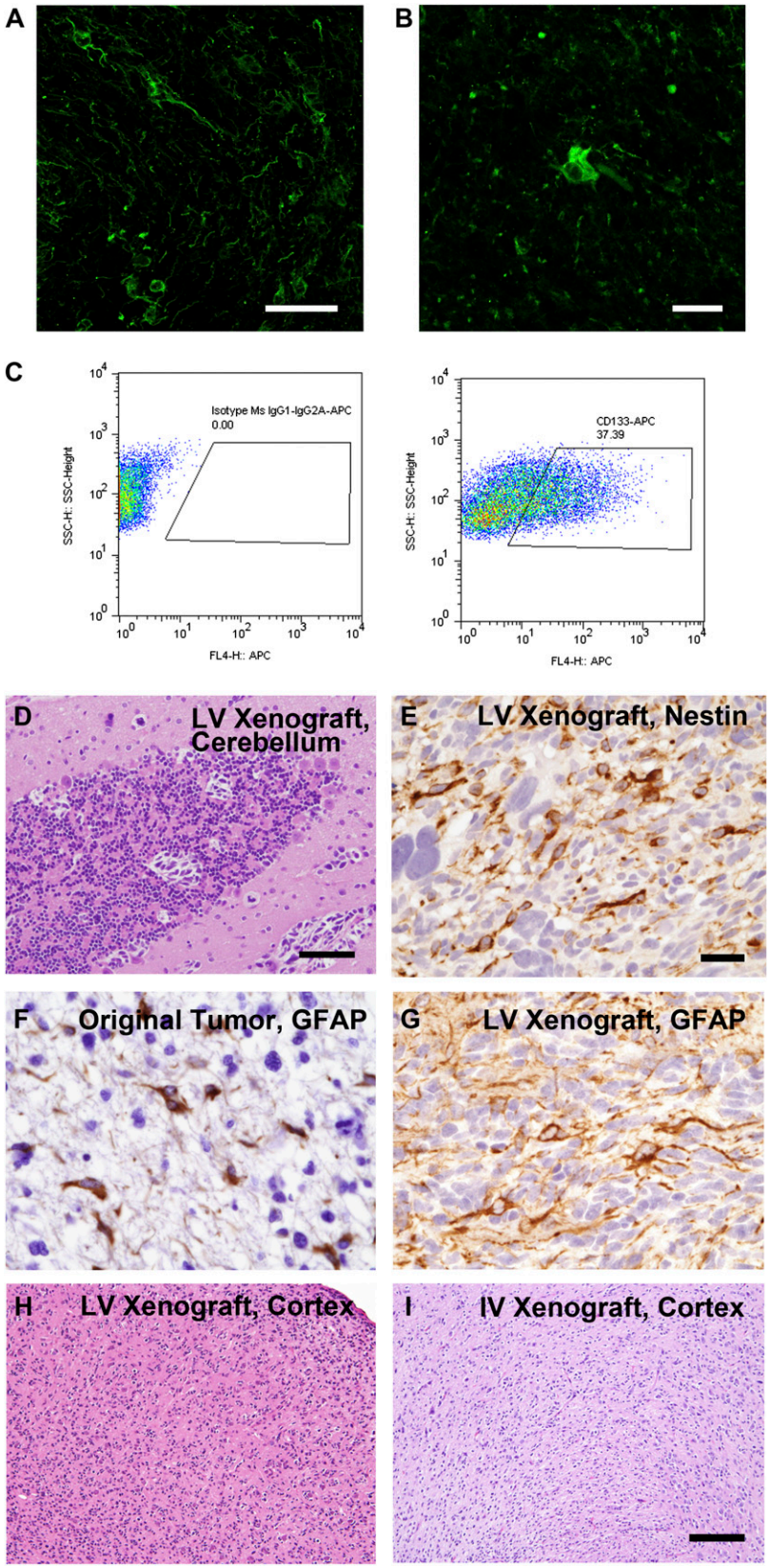

Fig. S3. Human DIPG neurosphere culture and xenograft models. Confocal photomicrographs (magnification 40×) showing Nestin (*A*, green) and CD133 (*B*, green) in the original tumor. (*C*) Tumor neurospheres were analyzed for CD133 expression using flow cytometry. (*Left*) As a control, background staining is shown by exposing cells to the appropriate Ig isotype directly conjugated to a fluorophore, in this case, mouse IgG1/IgG2B conjugated to APC. (*Right*) FACS analysis using mouse anti-human CD133/1 and anti-CD133/2 IgG1 that is directly conjugated to the fluorophore APC, revealing that 37% of cells express CD133. (*D*) Following stereotactic transplantation of dissociated neurospheres from a human DIPG into the LVs, examination of brains from immunodeficient mice

Legend continued on following page

reveals human tumor cells infiltrating the cerebellum (H&E stain, magnification 20×). (*E*) Nestin immunohistochemistry (brown) of xenograft (magnification 40×). Immunohistochemistry of the original tumor (*F*) and xenograft (*G*) reveals GFAP immunopositivity (magnification 40×). Diffuse infiltration of cortex following stereotactic transplantation to the LV (*H*) or IVth ventricle (*I*). (Scale bars: *A*, 50 μm; *B*, 20 μm; *D*, 100 μm; *E*–*G*, 50 μm; *H* and *I*, 250 μm.)

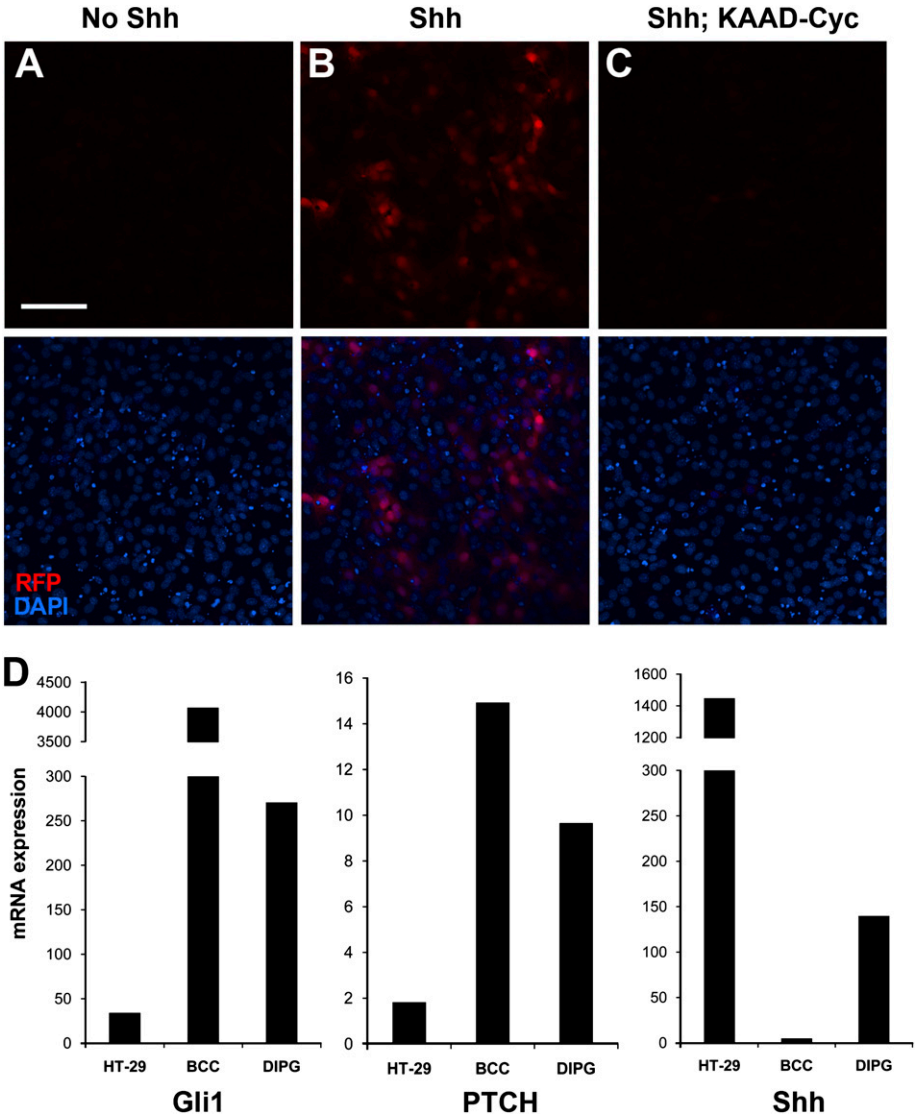

Fig. S4. Gli binding site-RFP reporter validation and RT-PCR. Confocal micrographs (z-stack projection images, magnification 20×) illustrating NIH 3T3 cells transduced with lentivirus containing Gli1 binding site::RFP construct. Cells were exposed to methanol vehicle control only (*A*), Shh-conditioned media (*B*), or Shh-conditioned media together with KAAD-cyclopamine (*C*, 200 nM) for 29 h; fixed with 4% (wt/vol) paraformaldehyde; and stained with the nuclear marker DAPI (blue, *Lower*). RFP expression is shown in red. (Scale bar: 100 μm.) (*D*) Fold change of mRNA expression for Gli1, PTCH1, and Shh normalized to DLD1^{-} control cells. DLD1 is used as a negative control for Shh ligand and Hh pathway activity as monitored by Gli1 and PTCH1. HT-29 cells are used as a positive control for Shh ligand, and primary human basal cell carcinoma (BCC) is used as a positive control for Hh pathway activity.